

Supplement 1

Text S1. Additional Methods

Text S1.1. Details of snail counting

Marine snail (*Littorina* spp.) populations living on basalt within the acorn barnacle (*Balanus glandula* Darwin, 1854) littoral zone were surveyed twice per year between 1993 and 2021 at two wave-exposed sites (Fig. 1 in the main article): Prasiola Point (PP) and Nudibranch Point (NP). The two sites were located on rocky outcrops at either end of a 400-m wave-exposed sandy beach (Fig. S1) between Bamfield Marine Sciences Centre, hereafter BMSC (48.835532°, –125.135478°) and the Cape Beale Lighthouse, hereafter CB (48.78617°, –125.2162°) on Vancouver Island, BC Canada (Fig. S1). The Vancouver Island study sites are separated from the Deer Group Islands by Trevor Channel which, drops off into Folger Passage (Fig. S2).

The original goal of the semi-annual surveys was to monitor the demographic and evolutionary responses of littorinid snail populations in response to an experimental increase in the local density of an indigenous predatory crab, the purple shore crab, *Hemigrapsus nudus* (Dana, 1851) (Boulding et al. 2007). The local *H. nudus* density was increased successfully by constructing concrete crab shelters between 1993 and 1998 (E.G. Boulding, unpubl. data). To monitor the response of the surrounding natural *Littorina* populations, a 30-m measuring tape was placed parallel to the shoreline on flat rocky intertidal areas covered by *B. glandula*. Vertical transects 1 m in length were created by placing a meter stick perpendicular to the measuring tape at different distances from the crab shelters. At random locations along each 1-m transect (PP: N = 6, NP: N = 7) were five 10-cm x 10-cm permanent quadrats marked with stainless steel screws.

All quadrats were counted once in July (either late July or the first half of August) and once in December (either late December or early January) if it was safe to do so. Here, counts from early January were classified as December counts from the previous year. Counting was done by using fine-point precision forceps (length ≈ 11.4 cm with serrated handles and tips) to remove all *Littorina* spp. larger than 1.0 mm in shell length from inside each permanent quadrat (Fig. S3). The removed snails were then placed inside a labelled, 150-mm-diameter round petri dish held together with elastic bands. Different rows of a 24-well cell culture plate with a matching label were then used to separate each species into size classes, beginning with the 1.5– 2.4-mm size class and ending with the largest size class for that species (Table S1). The number of individuals in each size class was then recorded before returning the snails to their original quadrat. From the earliest preliminary sampling in ‘October’ 1993 to the sampling in July 2009, the collection of snails from each quadrat in a particular transect, the sorting, the recording, and the replacement of the snails into their original quadrat was done at a study site during the same low tide. Sampling of all the transects at a site could take multiple days. However, beginning in December 2009, the snails from each quadrat of a particular transect were sorted in a BMSC laboratory, returned to their labelled petri dish, stored overnight in a refrigerator, and then returned to their original quadrat the following day. A benefit of laboratory sorting was that the two *Littorina* species with planktotrophic larvae could be distinguished under a dissecting scope depending on whether their tentacles had longitudinal (*L. plena*) or transverse (*L. scutulata*) dark stripes on them (Reid et al. 1996, Hohenlohe & Boulding 2001).

The same four indigenous species of *Littorina* were present at both sites. Common in wave-exposed quadrats was a round, thin-shelled DD species, Newcomb’s periwinkle, *L. subrotundata* (Carpenter, 1864), which becomes sexually mature at a shell length between 3.3 and 5.0 mm in males and 3.8 and 5.5 mm in females (Boulding et al. 1993). A second round DD species, the Sitka periwinkle, *L. sitkana*, Philippi, 1846, is distinguished by its thick, ridged shell and the black pigmentation of its body, has crawl-away juveniles that hatch from large communal attached egg masses (Buckland-Nicks et al. 1973) and becomes sexually mature at larger sizes (3.5–6.0 mm in males and 4.5–7.0 mm in females) (Boulding et al. 1993, Rochette et al. 2003). Two high-spined and thick-shelled PD species, the black periwinkle, *L. plena*, Gould, 1849, and the checkered periwinkle, *L. scutulata sensu stricto*, Gould, 1849, (Mastro et al. 1982, Reid et al. 1996) have distinctive planktonic floating egg capsules (Murray 1979, Strathmann 2023) that hatch into planktotrophic larvae that swim freely in the plankton for at least 5 weeks (Hohenlohe 2002). In California, female *L. plena* become sexually mature at a shell length of about 5 mm, whereas female *L. scutulata s.s.* become sexually mature at about 7 mm (Chow 1987, 1989). However, in Washington State, populations male and female *L. scutulata s.s.* may become sexually mature under 3 mm in shell length (Hohenlohe 2002).

I combined ‘small’ mostly juvenile snail size classes (shell lengths: 1.5–2.4 mm and 2.5–3.4 mm) by taxon before calculating their anomalies. ‘Large’ mostly adult snails (shell length greater than 3.4 mm) were also combined by taxon. The DD *L. subrotundata* was often abundant at wave-exposed study sites; however, its more wave-protected congener, the DD, *L. sitkana*, was rare at my open coast study sites PP and NP. In the current analysis, I combined the counts for the two PD species, *L. plena* and *L. scutulata sensu stricto* into one taxon, hereafter called ‘*L. scutulata sensu lato*’ count anomalies. Combining the counts of the two PD species, which can be distinguished only with a microscope, allowed me to include the count data from July 1994 to December 2009, when snails were counted on the shore rather than in the laboratory.

As I was primarily interested in discovering covariates that affected the recruitment of juveniles, the MARSS statistical modelling used only the log₁₀ count anomalies for the ‘small’ snails. Large snails were used as candidate covariates. One of the two DD species, *L. sitkana*, was rare to include in my MARSS modelling. Finally, to keep wave-exposure as constant as possible, I omitted counts from two transects at NP: 14.5 m because it was atypically wave protected and 20.0 m because it could not always be counted during winter storms. To keep anomaly estimates as precise as possible, this study included three wave-exposed transects within 1 m of the crab shelters (PP: 0.3 m and 0.6 m and NP 1.0 m). I also plotted a different subset of the dataset, which included the 14.5 m and 20.0 m transects at NP but did not include these three transects within 1 m of the crab shelters. The same temporal differences in abundance patterns between the DD *L. subrotundata* and PD *L. scutulata sensu lato* during very strong El Niño events were consistent regardless of which subset of the data was used.

Text S1.2. Snail predators

Male and female purple shore crabs (*Hemigrapsus nudus*) of carapace width (cw) 15–20 mm were collected from the Bamfield region and introduced into the openings of the crab shelters at PP and NP each July and December. The indigenous *H. nudus* has unspecialized claws, which results in a low feeding efficiency in the laboratory on *L. sitkana* (Behrens Yamada & Boulding 1998). Live snail tethering experiments show that *H. nudus* predation on *Littorina* spp. can be high within 1 m of a shelter but is low at transects further away (Boulding et al. 2007). Following the two extreme El Niño events (1997–1998 and 2015–2016) some of the crab shelters (and natural high intertidal crevices in the rock) contained the lined shore crab, *Pachygrapsus crassipes* until they died of old

age (Fig. 3 in the main article). The lined shore crab prefers the thinner-shelled *L. sitkana* over the thicker-shelled *L. scutulata* (Boulding et al. 2020). Any lined shore crabs present were removed from the shelters, measured, counted and then preserved in ethanol during the July sampling periods. Annual summer counts of shore crab abundance became more quantitative after 2018. Long forceps, pliers and a nail puller were used to remove all shore crabs from the concrete crab shelters. Crabs that were removed were identified to the species level and sexed, and their carapace width was measured with callipers. Individual lined shore crabs (*P. crassipes*) were preserved in 95% ethanol for later genetic studies (Cassone & Boulding 2006). Large purple shore crabs (*H. nudus*) of $cw > 20$ mm were replaced by freshly collected *H. nudus* ≤ 20 mm cw. This replacement was done because only small *H. nudus* exert selection differentials for increased shell thickness because of the thin shell of *Littorina subrotundata* (Pakes & Boulding 2010). The red rock crab and the pile perch (*Rhacochilus vacca*) are not important predators of *L. sitkana* on wave-exposed shores such as PP and NP (Boulding et al. 1999, 2001).

Text S1.3. Detailed statistical and modelling methods

S1.3.1. Details of anomaly calculations – Step 1 of the Interactive Spatiotemporal Data & Time Series Toolkit Time-series Explorer ‘NAUPLIUS’ provides oceanographic data hosted by NOAA as monthly anomalies for a selected point or points in the ocean. Step 2 of this Toolkit ‘COPEPODITE’ calculates anomalies for user-uploaded SST, wave height, windspeed, weather and invertebrate count datasets. The program calculates anomalies using the untransformed data values for uploaded temperature and salinity. However, the program calculates anomalies using are log₁₀ transformed values for uploaded plankton, chlorophyll, and nutrient values which it identifies by a special prefix before the variable name (e.g., ‘ABDT=’ for copepod counts where zero means no copepods were found. To avoid problems caused by log₁₀ transformation of values less than 1, the program replaces counts of zero by 50% of the lowest non-zero value in that data column (O’Brien et al. 2013, O’Brien & Oakes 2020). To obtain the anomalies, I uploaded my raw snail counts to the COPEPODITE website as separate columns for the groupings: life history (PD or DD) by season (July or December) by site (PP or NP) by snail size class (small or large) using variable names with the ‘ABDT=’ prefix. I also uploaded monthly means, minimums, and maximums for daily rainfall, minimum and maximum air temperature monthly data from the CB lighthouse, and from the Tofino airport using the appropriate prefixes. I also uploaded SST, wind speed and wave height monthly data from the La Perouse buoy (Table S2). COPEPODITE automatically calculated the ‘Monthly Climatology’ using the mean values for that month calculated over the baseline of all years for which data was uploaded. RATIO Anomalies, which are the Monthly Anomalies divided by the Monthly Climatology. The calculation of unitless log-transformed anomalies facilitates comparison of changes in the abundances of common species with those of rarer species (O’Brien et al. 2013). For my snail count columns, the COPEPODITE program calculated ‘Monthly Anomalies’, by subtracting the mean monthly count for a size class of a taxon averaged over 1994 to 2021 from the untransformed count for that size class of that taxon for that month. The COPEPODITE program calculated a third type, ‘Mackas’ Anomalies, hereafter ‘Log₁₀ anomalies’, by subtracting the log₁₀(x) of the mean monthly count over the baseline from the log₁₀(x) transformed counts for each year of a size class of a particular taxon. If a sampled quadrat was surveyed but had zero snails in it then for my uploaded snail count dataset, where one snail is the minimum non-zero value, the value became 0.5 to allow the log₁₀ transformation. Once ‘COPEPODITE’ had calculated the anomalies and generated plots of the anomalies for each variable, it was possible to download the transformed dataset.

In addition to uploading my snail counts to the ‘COPEPODITE’ website, I also wrote R-scripts (<https://cran.r-project.org>) using R-Studio (<http://www.rstudio.com/>) to calculate the three types of monthly anomalies for different groupings of my snail dataset.

S1.3.2. Non-collinear covariate subsets – Stepwise univariate multiple linear regressions through the origin were used to determine which of the often highly collinear oceanographic and environmental variables should be used in the MARSS models (IBM SPSS Statistics version 29.01). The dependent variable used for the stepwise regressions was the count anomalies for a particular set of Log10-transformed small snail anomalies (1.5–2.4-mm size classes combined). All 33 oceanographic, weather and biological variables (counts of small and large heterospecific *Littorina* species and counts of predatory lined shore crabs) were included as potential independent variables.

At each step, the independent variable with the smallest probability of F was automatically added to the regression model. Variables already in the regression equation were automatically removed if their probability of F became sufficiently large, which usually occurred because they were highly correlated with the newly entered variable. <https://www.ibm.com/docs/en/spss-statistics/29.0.0?topic=regression-linear-variable-selection-methods> Stepwise regressions were run separately for each life history (PD or DD) by season (July or December) by site (PP or NP) combination. *A priori* hypothesis-relevant covariate subsets that overlapped between the two sites were then used in all six classes of MARSS models.

S1.3.3. MARSS Model Classes 1–6. – I followed the methodology given in the r-script for Chapter 13 of the MARSS user manual ‘Incorporating covariates into MARSS models’ (Holmes et al. 2023). A total of six multivariate autoregressive state–space (MARSS) models were run for both sites (PP and NP) simultaneously using the subsets of covariates suggested by stepwise multiple regression analysis for all life history (PD or DD) by season (July or December) groupings of the Log10 snail count anomalies. The output from all six model classes for each subset of covariates – including the Akaike’s Information Criterion corrected for small sample size (AICc) and the ‘slope’ coefficients, standard error and 95% confidence limits for each covariate – were saved as separate text files for all four groupings. To find the consistently best model, the Δ AICc values were calculated as the difference between the AICc value for a particular model and the smallest AICc value observed for the other five models for a particular subset of covariates for each of the life history by season groupings. Once the best model was chosen, the first summary table was made showing the ‘slope’ coefficients for the subset of covariates that gave the lowest AICc value for a particular grouping. To facilitate the testing of the hypotheses, the ‘slope’ coefficients from a common subset of covariates was determined by creating a table that compared the rankings of all subsets of covariates for the life history by season groupings. This common subset of covariates was run using the chosen *state variable* model class for all four groupings and made into a second summary table. A third table reviewed the evidence for each *a priori* hypothesis.

Text S2. Additional Results

Text S2.1. Snail density changes for all four *Littorina* species

The four *Littorina* species differed in the abundances of their new recruits (shell length: 1.5–3.4 mm) per 10-cm × 10-cm quadrat at PP and NP between 1994 and 2021 (Table S1). The wave-exposed DD species, *L. subrotundata*, had the highest mean density (mean ± se: 2 mm: 6.986 ± 0.1937 and 3 mm: 5.581 ± 0.1286, N = 3419) averaged over both sites during July and December. The wave-protected

DD species, *L. sitkana*, was much rarer at PP and NP (2 mm: 0.0895 ± 0.009253 and 3 mm: 0.1682 ± 0.01176 , $N = 3419$). Beginning in December 2009 when the two planktotrophic species were counted separately, the mean density of the combined 2- and 3-mm size classes of *L. plena* (1.56 ± 0.084 , $N = 1547$, Kruskal-Wallis, $p < 0.001$) was significantly greater than that for *L. scutulata s.s.* (0.65 ± 0.042 , $N = 1547$, Kruskal-Wallis, $p < 0.001$).

Text S2.2. Responses to extreme El Niño – parametric statistics

The small PD snails increased in abundance during very strong El Niño events. The mean positive anomaly for small PD *L. scutulata s.l.* (mean \pm se: 0.4054 ± 0.31627 , $N = 8$) during the 1997–1998 El Niño event was significantly larger (ANOVA, $df = 1, 15$, $p = 0.002$) than that for small DD *L. subrotundata* (mean \pm se: 0.1065 ± 0.21475 , $N = 8$). The same was true for the PD ‘large’ snails during the 1997–1998 El Niño event (ANOVA, $df = 1, 15$, $p = 0.002$). Similarly, during the 2015–2016 very strong El Niño event, the mean positive anomaly for small PD *L. scutulata s.l.* (mean \pm se: 0.4891 ± 0.20930 , $N = 8$) was significantly larger than that for small DD *L. subrotundata* (0.2549 ± 0.23861 , $N = 8$; ANOVA, $df = 1, 15$, $p < 0.001$). The same was true for the large PD snails during the 2015–2016 strong El Niño event (ANOVA, $df = 1, 15$, $p < 0.001$).

By contrast, the DD snail increased in abundance during the years (2005–2013) without very strong El Niño events. The small PD *L. scutulata s.l.* (-0.2470 ± 0.14175 , $N = 35$), showed a negative count anomaly that was significantly (ANOVA, $df = 1, 69$, $p < 0.001$) smaller than the positive count anomaly for the small DD *L. subrotundata* (0.226 ± 0.222 , $N = 35$). The same pattern was true of the large snails. The PD *L. scutulata s.l.* (-0.340 ± 0.183 , $N = 35$), had a negative count anomaly that was significantly (ANOVA, $df = 1, 69$, $p < 0.001$) smaller than the positive count anomaly shown than the *L. subrotundata* ($0.04419 \pm .20961$, $N = 35$). The nonparametric independent-samples Mann-Whitney U Test analyses with species as the predictor variable confirmed the parametric univariate ANOVA results in all cases (Section 3.1.2 of main manuscript).

Text S2.3. MARSS model class and covariate selection

For a given set of covariates, the MARSS *State variable* (Table S3 model 13.4c: process-error only, autoregressive and mean-reverting with the initial states determined by the data at time = 1, error only) model nearly always fit better than the MARSS *observation error only* model class (equivalent to multivariate linear regression, Table S3 model 13.3a). The AICc values for the best fitting subset of covariates for each life history by site grouping from the state variable model (Table 1 in the main article; Tables S6–S9), were much smaller than those for the same subset of covariates for the same grouping from the *observation error model* (data not shown). The AICc values were also smaller when for the best fitting subset of covariates for the *state variable* model for each grouping was compared to the best fitting subset of covariates for the *observation error only* model (data not shown). These two models always converged provided the subset of covariates that were used were not highly collinear (data not shown).

For the same subset of covariates, the MARSS *observation error only* model class, the two other *state variable* model classes (Table S3 models 13.4a–b) and the two model classes that had equations for both state variable process and observation error (Table S3 models 13.5a–b) consistently gave larger AICc values for each grouping than the *state variable* model presented above (Table S3 model 13.4c). Models 13.5a–b had more parameters and sometimes failed to converge. Therefore, I chose to use only the *state variable model* (Table S3, model 13.4c) in section 3.4 of the main manuscript.

Literature Cited

- Behrens Yamada S, Boulding EG (1998) Claw morphology, prey size selection and foraging efficiency in generalist and specialist shell-breaking crabs. *J Exp Mar Biol Ecol* 220:191–211.
- Boulding EG, Behrens Yamada S, Schooler SS, Shanks AL (2020) Periodic invasions during El Niño events by the predatory lined shore crab (*Pachygrapsus crassipes*): Forecasted effects of its establishment on direct-developing indigenous prey species (*Littorina* spp.). *Can J Zool* 98:787–797.
- Boulding EG, Buckland-Nicks J, Van Alstyne Katherine L. (1993) Morphological and allozymic variation in *Littorina sitkana* and related *Littorina* species from the northeastern Pacific. *Veliger* 36:43–68.
- Boulding EG, Hay T, Holst M, Kamel S, Pakes D, Tie AD (2007) Modelling the genetics and demography of step cline formation: Gastropod populations preyed on by experimentally introduced crabs. *J Evol Biol* 20:1976–1987.
- Boulding EG, Holst M, Pilon V (1999) Changes in selection on gastropod shell size and thickness with wave-exposure on northeastern Pacific shores. *J Exp Mar Biol Ecol* 232:217–239.
- Boulding EG, Pakes D, Kamel S (2001) Predation by the pile perch, *Rhacochilus vacca*, on aggregations of the gastropod *Littorina sitkana*. *J Shellfish Res* 20:403–409.
- Buckland-Nicks J, Chia FS, Behrens S (1973) Oviposition and development of two intertidal snails, *Littorina sitkana* and *Littorina scutulata*. *Can J Zool* 51:359–365.
- Cassone BJ, Boulding EG (2006) Genetic structure and phylogeography of the lined shore crab, *Pachygrapsus crassipes*, along the Northeastern and Western Pacific coasts. *Mar Biol* 149:213–226.
- Chow V (1989) Intraspecific competition in a fluctuating population of *Littorina plena* Gould (Gastropoda: Prosobranchia). *J Exp Mar Biol Ecol* 130:147–165.
- Chow V (1987) Patterns of growth and energy allocation in northern California populations of *Littorina* (Gastropoda: Prosobranchia). *J Exp Mar Biol Ecol* 110:69–89.
- Hohenlohe PA (2002) Life history of *Littorina scutulata* and *L. plena*, sibling gastropod species with planktotrophic larvae. *Invertebrate Biology* 121:25–37.
- Hohenlohe PA, Boulding EG (2001) A molecular assay identifies morphological characters useful for distinguishing the sibling species *Littorina scutulata* and *L. plena*. *J Shellfish Res* 20:453–457.
- Holmes EE, Ward EJ, Scheuerell M. D. (2023) Analysis of multivariate time-series using the MARSS package version 3.11.7. <https://atsa-es.github.io/MARSS/articles/index.html>
- Mastro E, Chow V, Hedgecock D (1982) *Littorina scutulata* and *Littorina plena*: Sibling species status of two prosobranch gastropod species confirmed by electrophoresis. *Veliger* 24:239–246.
- Murray TE (1979) Evidence for an additional *Littorina* species and a summary of the reproductive biology of *Littorina* from California. *The Veliger* 21 21:469–474.
- O'Brien TD, Oakes SA (2020) Visualizing and exploring zooplankton spatio-temporal variability. In: *Zooplankton Ecology*, 1st ed. Teodosio MA, Branco-Barbosa AM (eds) CRC Press, Boca Raton, p 192–224

- O'Brien TD, Wiebe PH, Falkenhaus T (2013) ICES Zooplankton Status Report 2010/2011
<https://wgze.net/zooplankton-status-report>.
- Pakes D, Boulding EG (2010) Changes in the selection differential exerted on a marine snail during the ontogeny of a predatory shore crab. *J Evol Biol* 23:1613–1622.
- Reid DG, Rumbak E, Thomas RH (1996) DNA, morphology and fossils: phylogeny and evolutionary rates of the gastropod genus *Littorina*. *Philos Trans R Soc Lond B Biol Sci* 351:877–895.
- Rochette R, Dunmall K, Dill LM (2003) The effect of life-history variation on the population size structure of a rocky intertidal snail (*Littorina sitkana*). *J Sea Res* 49:119–132.
- Strathmann RR (2023) Perils of drifting encapsulated embryos of the periwinkle *Littorina scutulata* from failures at launch and unscheduled landings. *Mar Ecol Prog Ser* 703:109–124.

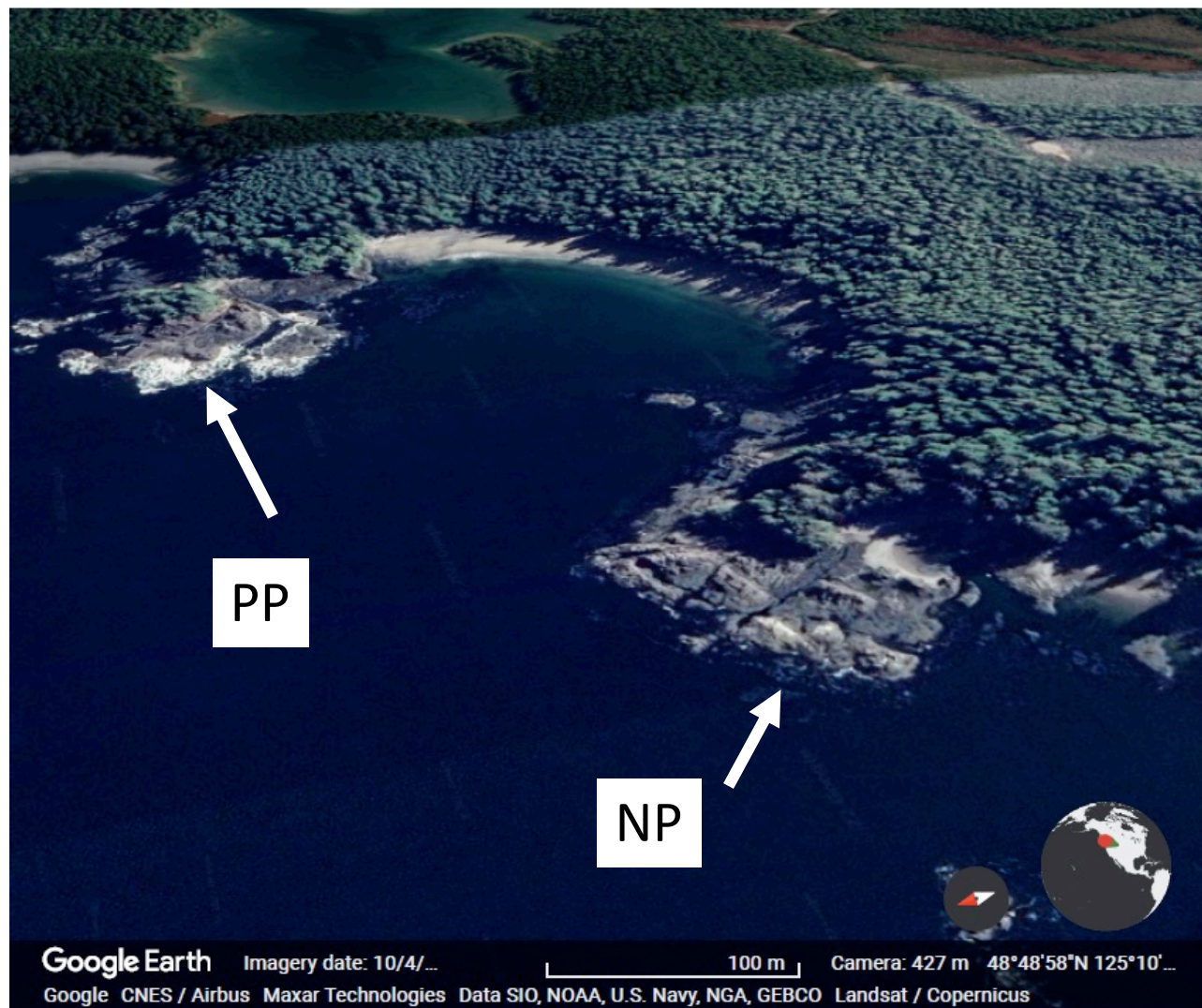


Fig. S1 The two study sites were at the east and west ends of Second Beach along the Cape Beale Peninsula near Bamfield, BC, Canada facing Trevor Channel (see Fig. 1 in the main article). Their latitudes and longitudes are 48.81710, -125.16964 for Prasiola Point (PP) and 48.815160, -125.175473 for Nudibranch Point (NP). Custom map was generated by Google Earth.

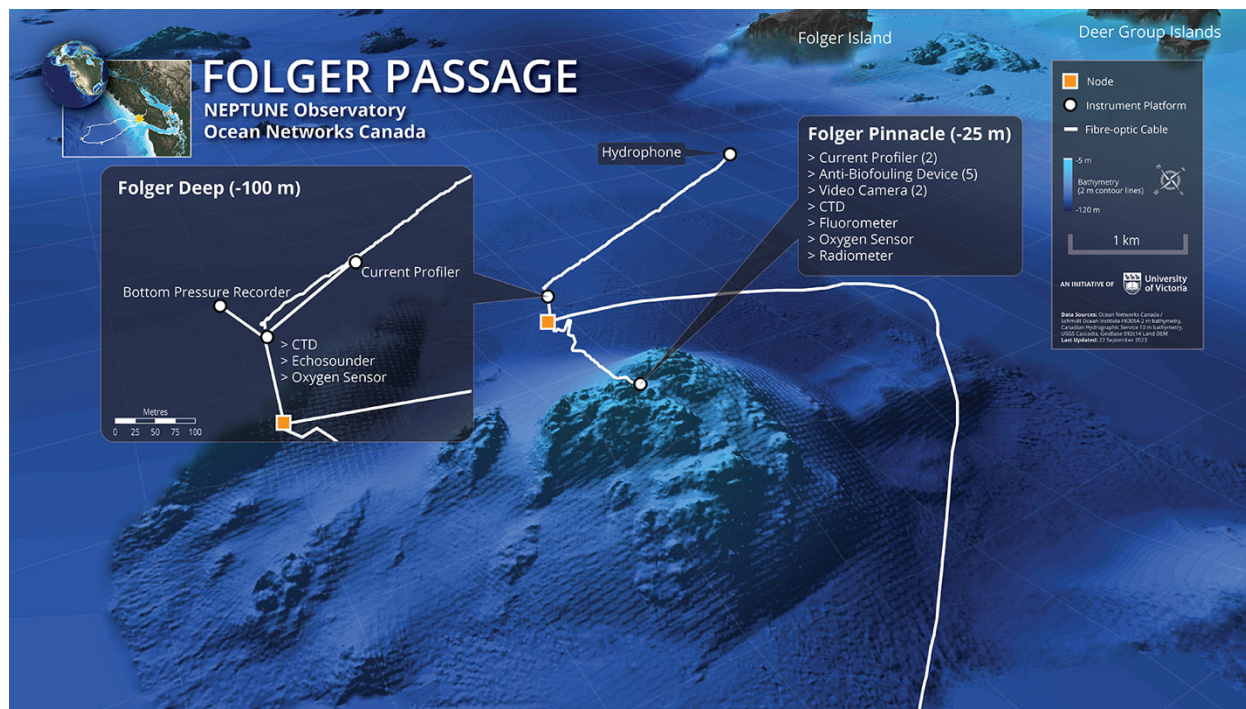


Fig. S2 Bathymetric image showing sea floor of Folger Passage at the entrance to Trevor Channel, which divides the Deer group of Islands from the Cape Beale Peninsula in Barkley Sound (see Fig. 1 in the main article). Two observatory sites belonging to Ocean Networks Canada are shown: Folger Deep (depth $\cong 100$ m) and Folger Pinnacle (depth 25 m), which are connected to a land-based shore station by a fibre optic cable. <https://www.oceannetworks.ca/multimedia/maps/>



Fig. S3 Wire frame (10 cm x 10 cm) used for collecting snails from then returning them to the same permanent quadrat. Side-cropped image (5472 x 3648 pixels) shows two species of acorn barnacles (large: *Balanus glandula*, small: *Chthamalus dalli* Pilsbry, 1916) and the fingered limpet (*Lottia digitalis* (Rathke, 1833)). Inside the quadrats are up to four species of *Littorina*: two species with high-spired shells (*L. scutulata sensu stricto* and *L. plena*) have floating egg capsules that hatch into a weakly swimming planktotrophic larval stage, and two species have round shells (*L. subrotundata* and *L. sitkana*) that have direct development from benthic egg masses. Yellow arrowheads show the snails (*Littorina* spp.) inside the quadrat that are in focus. The stainless-steel screw covered with red tech pen ink permanently marks the quadrat position.

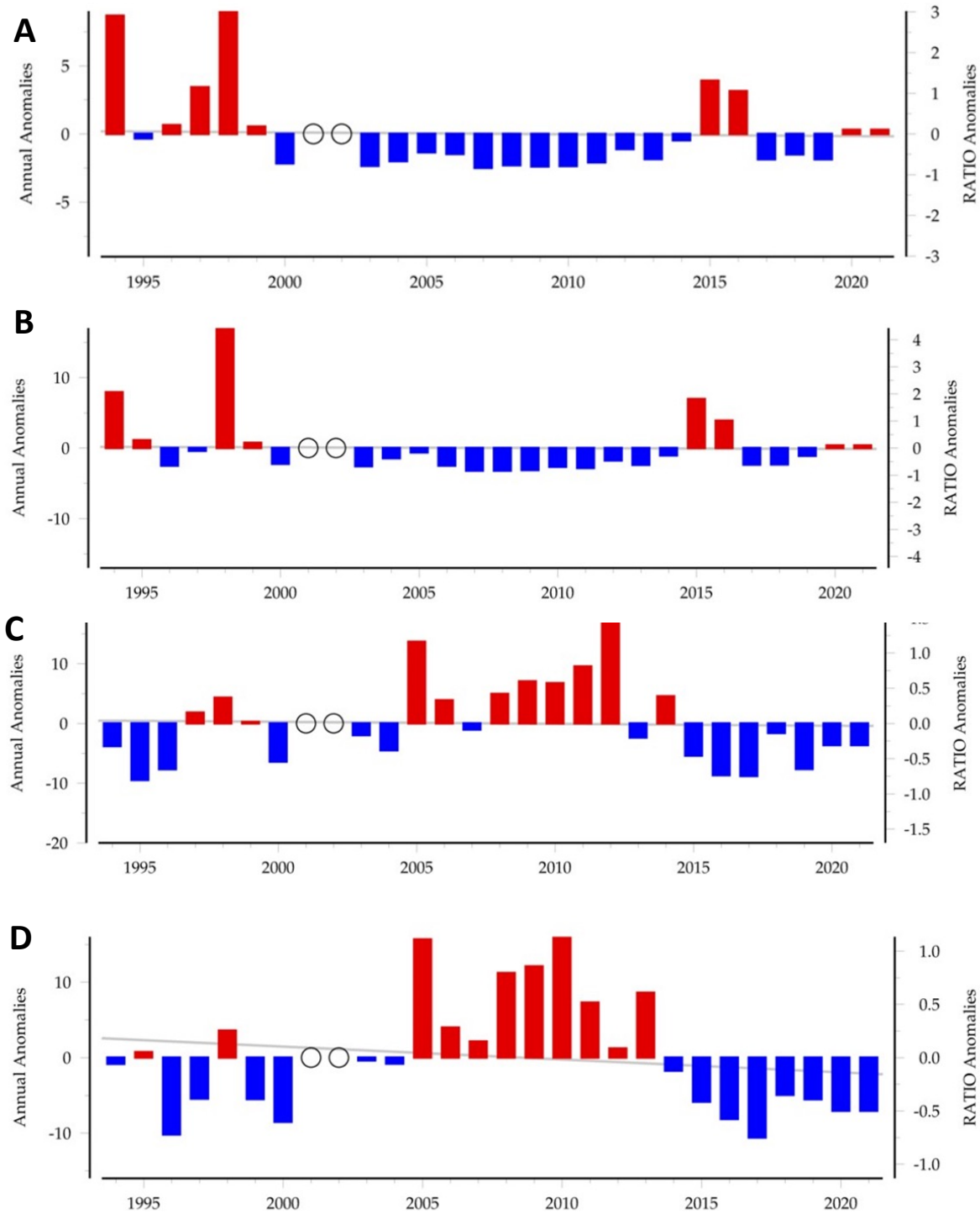


Fig. S4 Annual July and ratio count anomalies for newly recruited ‘small’ *Littorina* spp. (shell lengths 1.5-3.4 mm) automatically calculated and plotted using NOAA’s COPEPODITE Time Series Toolkit: slope thin gray line $p > 0.05$. [O] indicates a year where no July sampling was done. **(A)** *L. scutulata sensu lato* PP, **(B)** *L. scutulata s. l.* NP, **(C)** *L. subrotundata* PP, **(D)** *L. subrotundata* NP.

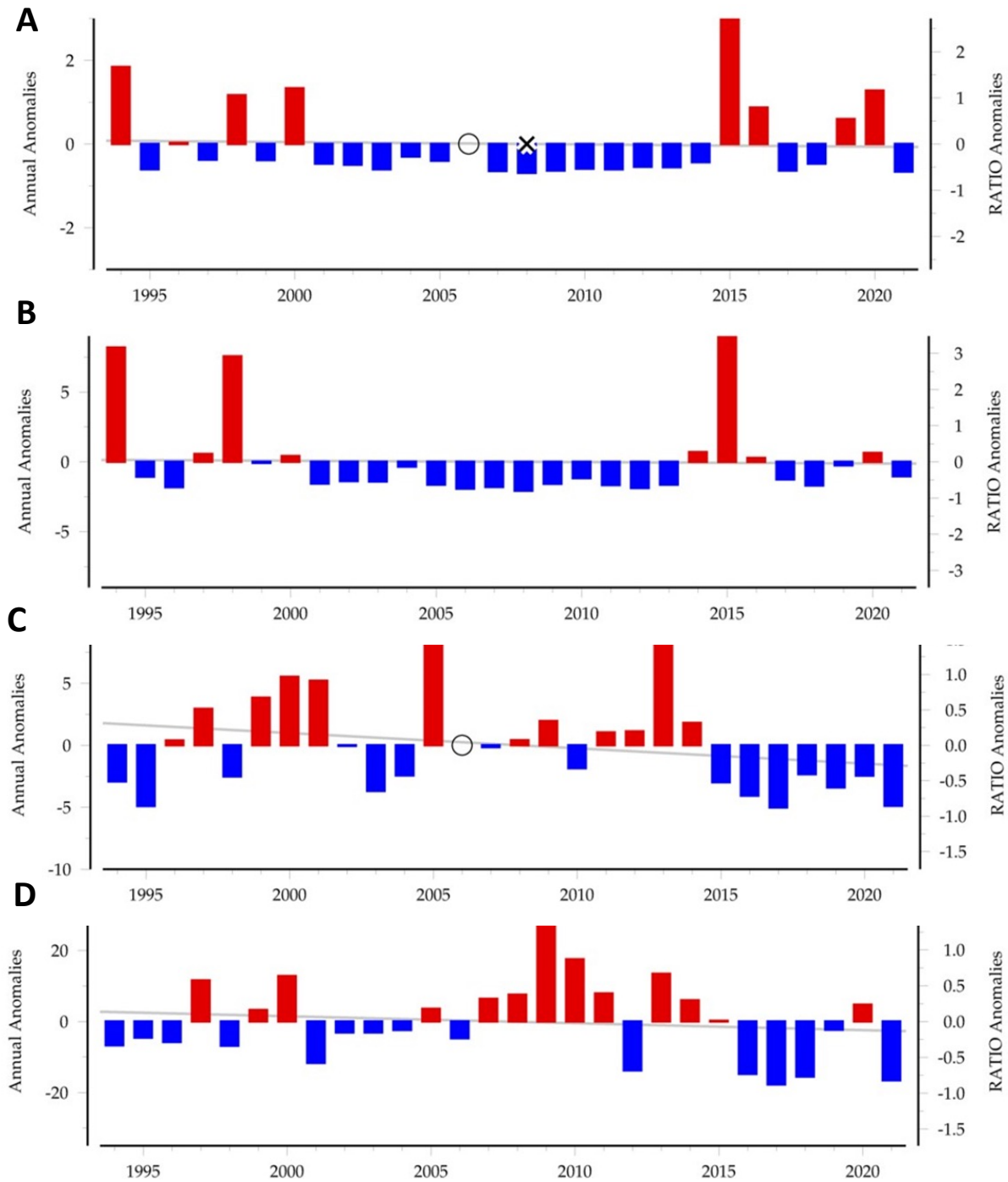


Fig. S5 Annual December and ratio count anomalies for newly recruited ‘small’ *Littorina* spp. (shell lengths 1.5-3.4 mm) automatically calculated and plotted using NOAA’s COPEPODITE Time Series Toolkit: slope thin gray line $p > 0.05$. [O] indicates a year where no "December" sampling was done. [X] indicates a year sampled where zero individuals were found. **(A)** *L. scutulata sensu lato* PP, **(B)** *L. scutulata s. l.* NP, **(C)** *L. subrotundata* PP, **(D)** *L. subrotundata* NP.

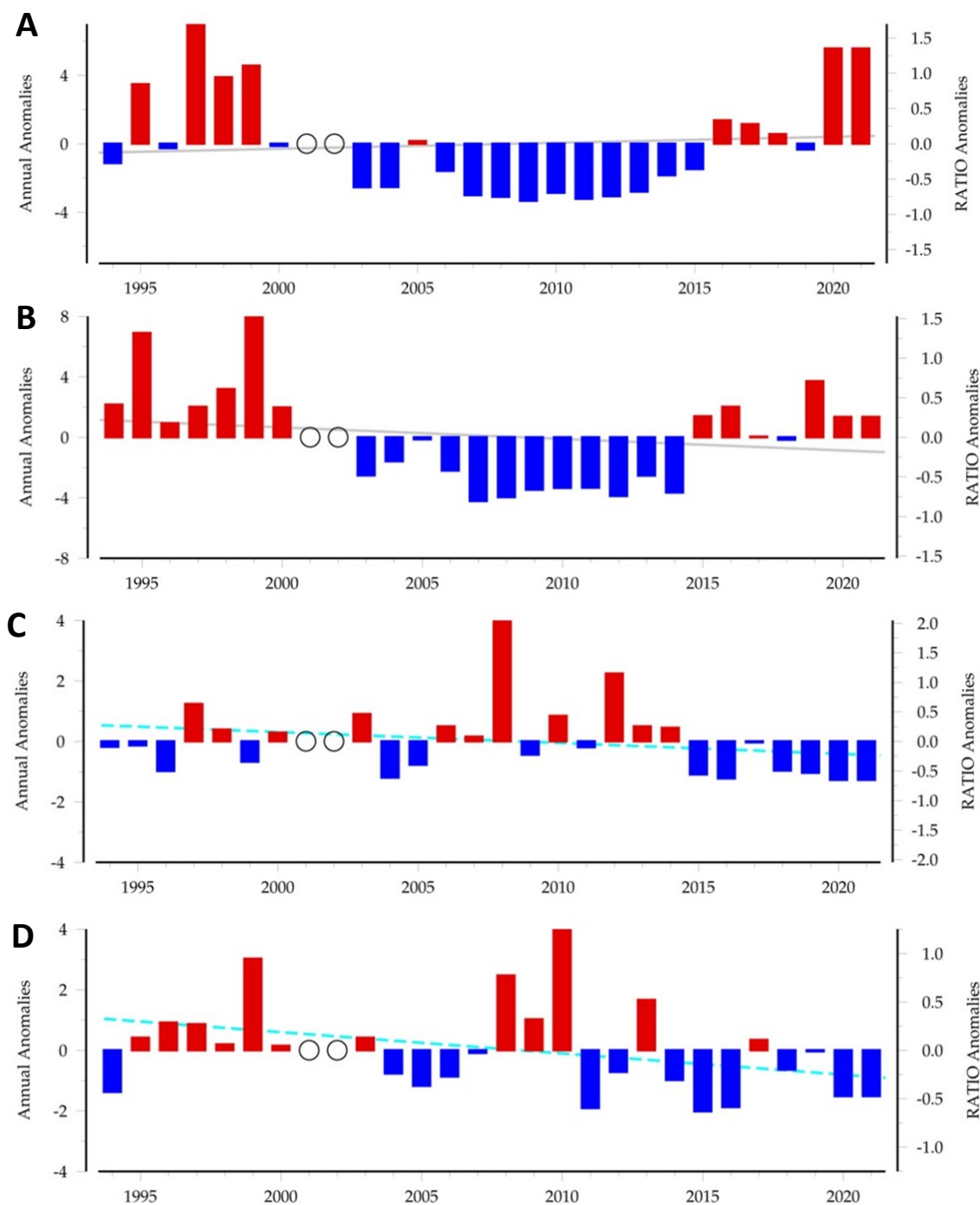


Fig. S6 Annual July and ratio count anomalies for adult ‘large’ *Littorina* spp. (shell length >3.4 mm) automatically calculated and plotted using NOAA’s COPEPODITE Time Series Toolkit: slope dashed blue line $p < 0.05$. [O] indicates a year where no July sampling was done. (A) *L. scutulata sensu lato* PP, (B) *L. scutulata s. l.* NP, (C) *L. subrotundata* PP, (D) *L. subrotundata* NP.

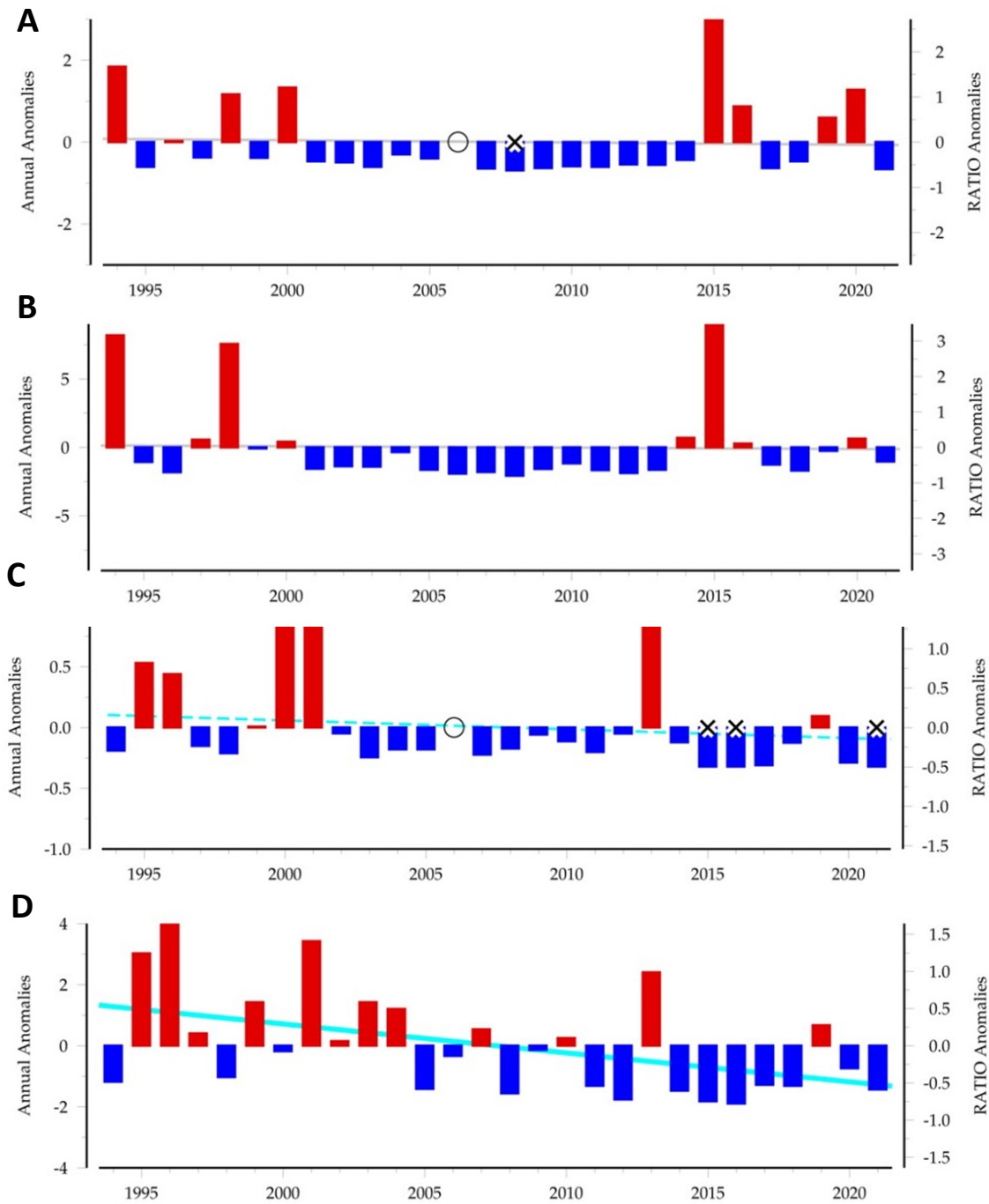


Fig. S7 Annual December and ratio count anomalies for adult ‘large’ *Littorina* spp. (shell length >3.4 mm) automatically calculated and plotted and using NOAA’s COPEPODITE Time Series Toolkit: slope dashed blue line $p < 0.05$, solid blue line $p < 0.01$. [O] indicates a site where no "December" sampling was done. [X] indicates a year sampled where zero individuals were found. (A) *L. scutulata sensu lato* PP, (B) *L. scutulata s. l.* NP, (C) *L. subrotundata* PP, (D) *L. subrotundata* (NP).

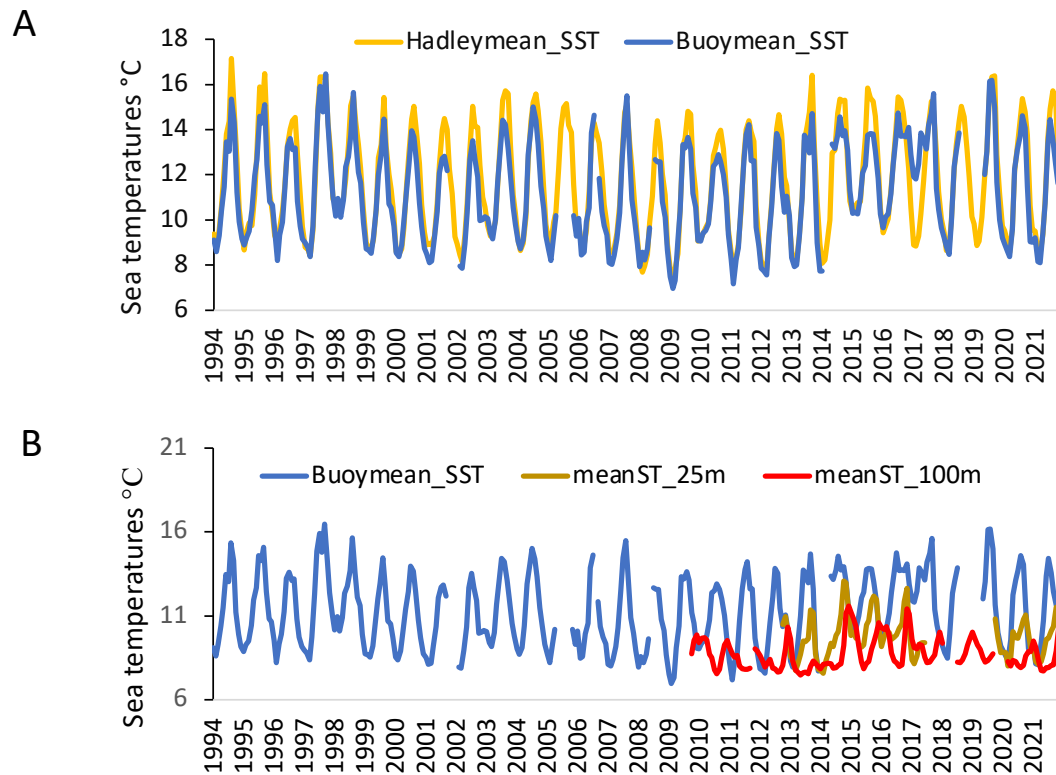
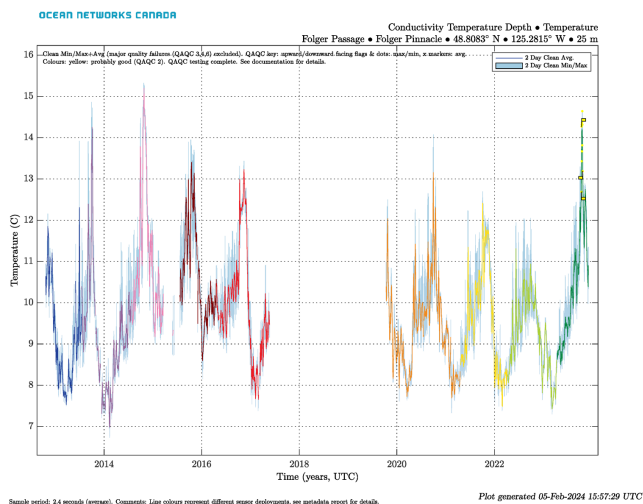


Fig. S8 Surface and subsurface sea water temperatures. **(A)** Mean Hadley satellite sea surface temperature (SST) and mean LP Buoy SST **(B)** mean LP Buoy SST and Ocean Networks Canada (ONC) subsurface sea temperatures at 25 m and 96.1 m. See Fig. 1 for map of locations of LP Buoy and ONC Folger underwater observatories. Fig. S2 shows a bathymetric image of the sea floor of Folger Passage with the location of ONC subsurface instrument panels at Folger Pinnacle (25m) and Folger Deep (96m). Fig. S9 shows time intervals with missing sea water temperature data from these two ONC observatories.

A



B

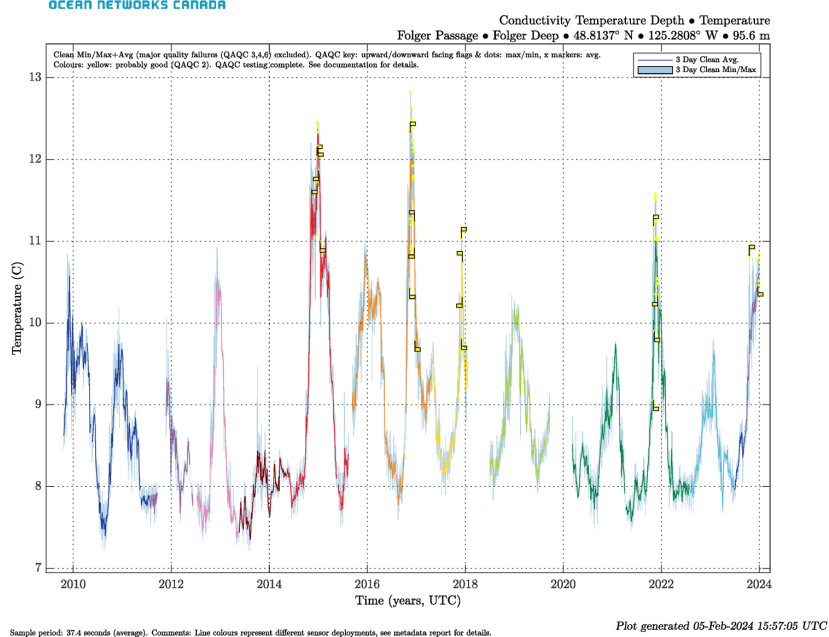


Fig. S9 Sea subsurface temperatures (°C) between Fall 2009 and December 2021 (blanks indicate time intervals with missing data) at **A**, Folger Pinnacle (depth 25 m), **B**, Folger Deep (depth 96.1 m) cable instrument platforms at the entrance to Barkley Sound. Major grid lines indicate January 1st biannually. Figures downloaded directly from Ocean Networks Canada (ONC).

<https://data.oceannetworks.ca/DataSearch?locationCode=FGPPN&deviceCategoryCode=CTD>

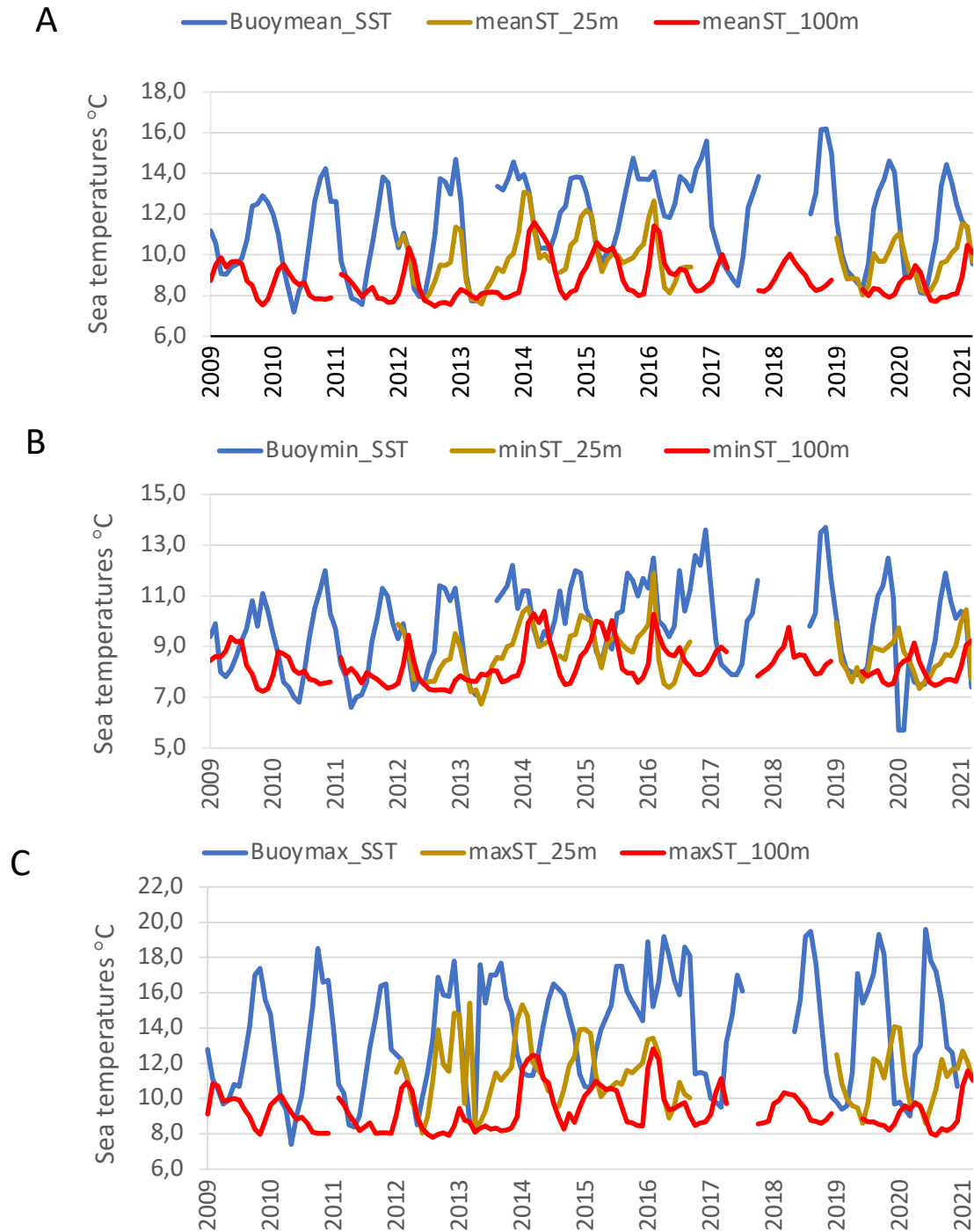


Fig. S10 Monthly sea water temperatures (°C) between October 2009 and December 2021 from La Perouse moored Buoy (surface), ONC Folger Pinnacle (depth 25 m), ONC Folger Deep (depth 96.1 m). A. monthly means, B. monthly minimums, C. monthly maximums.

Table S1. Descriptive statistics for raw counts of four different *Littorina* species per 10-cm × 10-cm permanent quadrat combined for both sites and both seasons for all years (1994–2021).

Species & size class ^a	Mean	SD	N, quadrats	SE	Maximum count per quadrat	Size-class % of species mean
sub2	6.985961	11.32474	3419	0.193677	106	47.74
sub3	5.581457	7.521377	3419	0.128632	111	38.14
sub4	1.820415	3.048839	3419	0.052142	29	12.44
sub5	0.320854	0.891909	3419	0.015254	12	2.19
sub6	0.047382	0.277034	3419	0.004738	5	0.32
sub7	0.004972	0.074391	3419	0.001272	2	0.03
sub8	0.000877	0.029613	3419	0.000506	1	0.01
sc2	0.541679	1.714292	3419	0.029318	31	7.22
sc3	2.156771	4.464605	3419	0.076354	57	28.76
sc4	2.598421	4.036972	3419	0.069041	43	34.65
sc5	1.458906	2.577357	3419	0.044078	29	19.45
sc6	0.454226	1.114507	3419	0.01906	14	6.06
sc7	0.133957	0.535637	3419	0.009161	8	1.79
sc8	0.058497	0.339647	3419	0.005809	8	0.78
sc9	0.021644	0.231007	3419	0.003951	9	0.29
sc10	0.008774	0.187166	3419	0.003201	10	0.12
si2	0.0895	0.541062	3419	0.009253	15	16.82
si3	0.168178	0.687661	3419	0.01176	10	31.61
si4	0.144779	0.608919	3419	0.010414	12	27.21
si5	0.075753	0.378388	3419	0.006471	8	14.24
si6	0.030418	0.204425	3419	0.003496	4	5.72
si7	0.011114	0.107607	3419	0.00184	2	2.09
si8	0.004095	0.063869	3419	0.001092	1	0.77
si9	0.003217	0.056638	3419	0.000969	1	0.60
si10	0.00117	0.034189	3419	0.000585	1	0.22
pl2	0.265029	1.086593	1547	0.027626	17	6.35
pl3	1.328378	2.722526	1547	0.069219	30	31.81
pl4	1.58565	3.086024	1547	0.078461	32	37.97
pl5	0.793148	1.881655	1547	0.04784	20	18.99
pl6	0.156432	0.566499	1547	0.014403	7	3.75
pl7	0.014867	0.131314	1547	0.003339	2	0.36
pl8	0.002586	0.0508	1547	0.001292	1	0.06
pl9	0.000646	0.025425	1547	0.000646	1	0.02
pl10	0	0	1547	0	0	0.00
st2	0.083387	0.440689	1547	0.011204	7	3.37
st3	0.563672	1.451786	1547	0.036911	14	22.78
st4	0.8649	1.850276	1547	0.047043	30	34.95
st5	0.550743	1.169571	1547	0.029736	12	22.26

st6	0.226244	0.658713	1547	0.016748	6	9.14
st7	0.079509	0.475275	1547	0.012084	8	3.21
st8	0.023917	0.206798	1547	0.005258	4	0.97
st9	0.008403	0.234329	1547	0.005958	9	0.34
st10	0.003878	0.062177	1547	0.001581	1	0.16

^a Variable name abbreviations: Suffixes: 1–10 refer to size class determined by measuring the shell length in mm (see Methods). Prefixes: sub = *L. subrotundata*, sc = *L. scutulata sensu lato* which represents *L. scutulata sensu stricto* and *L. plena* combined counts (field counts before December 2009), si = *L. sitkana*. Note that pl = *L. plena*, st = *L. scutulata sensu stricto* were distinguished by examining their tentacles with a dissecting microscope beginning with the December 2009 permanent quadrat counts.

Table S2. Oceanographic and coastal environmental variables were obtained from publicly available databases. Monthly averages were calculated using R scripts. Monthly averages for b-d were uploaded to NAUPLIUS to calculate monthly climatology using the baselines below. Monthly anomalies were then downloaded from COPEPODITE.

Name	Baselines used	Frequency	URL
NAUPLIUS ^a	1992–2021	Monthly	https://www.st.nmfs.noaa.gov/copepod/toolkit/subform_copepodite-c2.html
COPEPODITE ^a	1992–2021	Monthly anomalies	https://www.st.nmfs.noaa.gov/copepodite/
LP Buoy C46206 ^b	1993–2021	Hourly	https://www.pac.dfo-mpo.gc.ca/science/oceans/data-donnees/buoydata-donneebouee/index-eng.html#buoy-locations-and-data
CB lighthouse ^c	1993–2021	Daily	https://www.canada.ca/en/environment-climate-change/services/general-marine-weather-information/understanding-forecasts/decode-information-lighthouse-reports.html
Tofino Airport ^d	1992–2021	Daily	https://climate.weather.gc.ca/climate_data/daily_data_e.html?StationID=52960
Surface currents ^e	N/A	Monthly	https://cordc.ucsd.edu/projects/hfrnet/#
Subsurface Seawater Temperatures ^f	N/A	Each second	https://data.oceannetworks.ca/DataSearch?locationCode=FGPPN&deviceCategoryCode=CTD

^a NAUPLIUS Spatiotemporal Data Toolkit provided Hadley Sea Surface Temperature (SST), Hadley EN4 Salinity S at 5 m (Good & Rayner 2013), International Comprehensive Ocean-Atmosphere Data Set (ICOADS) scalar windspeed for 1994–2021, and combined NASA satellite ocean chlorophyll data for 1998–2021 for a 50-km × 50-km region defined by the latitude and longitude that I specified of 48.78059388872995, –125.24307250976561 (see Fig. 1 in the main article). COPEPODITE calculated and plotted the monthly anomaly for each variable usually based on its average value for July and for December that had been calculated using the 1992–2021 time series baseline.

^b Canadian Coast Guard Buoy C46206 - La Perouse Bank (see Fig. 1 in the main article, 48.844 N 126.010 W) measures daily sea surface temperature, maximum wave height and windspeed). Buoy C46206 floats at the surface and is moored to an anchor at a depth of 73 m. Buoy data interpretation information at <https://www.canada.ca/en/environment-climate-change/services/general-marine-weather-information/understanding-forecasts/decode-information-lighthouse-reports.html> [Buoy is 58 km from Cape Beale lighthouse and 32 km from Tofino Airport <https://www.nhc.noaa.gov/gccalc.shtml>].

^c Environment Canada CAPE BEALE LIGHT 1031316 (lighthouse), elevation 60 m (see Fig. 1 in the main article, 48.7865° N, 125.2155° W). Maximum and minimum daily air temperature and approximate total daily rainfall were downloaded via the Pacific Climate Impacts Consortium (PCIC) <https://pacificclimate.org/data/bc-station-data-disclaimer> [52 km from Tofino Airport <https://www.nhc.noaa.gov/gccalc.shtml>]

^d Environment Canada TOFINO airport 1038205 Hourly temperatures since 2014, daily before) Tofino Airport weather station (see Fig. 1 in the main article, 49.07913°N, 125.77569 °W, elevation 24 m. <https://pacificclimate.org/data/bc-station-data-disclaimer>

^e HF-Radar Real-Time Surface Currents. (Exported direction and speed monthly averages for January and for July for 2012–2021 were obtained from the ‘Near Real-Time Surface Current’ vectors produced from data collected by the open coast HF-Radar Network Stations at Westport State Park WA (46.9027°, –124.1316°) and at Loomis Lake, OR (46.4333°, –124.0589°). No anomalies were calculated because the baseline was too short to use in the MARSS time-series modelling).

^f Ocean Networks Canada Subsurface Seawater Temperatures (Fig. 1 in the main article, S1): Folger Deep (depth 96 m, from Fall 2009 to December 2021) and Folger Pinnacle (depth 25 m, available from Fall 2012 to Fall 2017 and then from Fall 2019 to December 2021). No anomalies were calculated because the baseline was too short to use here).

Table S3. Six classes of multivariate Autoregressive State-Space (MARSS Equations used in time series analyses with covariates (Holmes et al. 2023). MARSS uses an Expectation-Maximization (EM) algorithm for maximum likelihood estimation in the presence of state variables, \mathbf{x} , the true snail abundances (process), which are not measured directly, and observations, \mathbf{y} , are the snail count data used to estimate the state variables*. The Complete General Model is:

$$\mathbf{x}_t = \mathbf{B}_t \mathbf{x}_{t-1} + \mathbf{u}_t + \mathbf{C}_t \mathbf{c}_t + \mathbf{w}_t, \text{ where } \mathbf{w}_t \sim \text{MVN}(0, \mathbf{Q}_t) \quad (1)$$

$$\mathbf{y}_t = \mathbf{Z}_t \mathbf{x}_t + \mathbf{a}_t + \mathbf{D}_t \mathbf{d}_t + \mathbf{v}_t, \text{ where } \mathbf{v}_t \sim \text{MVN}(0, \mathbf{R}_t) \quad (2)$$

where: \mathbf{B}_t is a matrix containing autoregressive coefficients for $m \times 1$ state vectors \mathbf{x}_t , and \mathbf{x}_{t-1} , that estimate the effect of the abundance of each snail species at time $t - 1$ based on its abundance at time t . \mathbf{Z}_t is a matrix containing a coefficient giving the relationship between the observed snail abundances, $m \times 1$ state vectors \mathbf{x}_t , and their actual abundances, $n \times 1$ observation vector \mathbf{y}_t . \mathbf{c}_t is the $p \times 1$ vector of covariates (e.g. temperature, rainfall), which affect the states and \mathbf{d}_t is a $q \times 1$ vector of covariates (potentially the same as \mathbf{c}_t , which affect the observations. \mathbf{C}_t is an $m \times p$ matrix of coefficients relating the effects of \mathbf{c}_t to the $m \times 1$ state vector \mathbf{x}_t , and \mathbf{D}_t is an $n \times q$ matrix of coefficients relating the effects of \mathbf{d}_t to the $n \times 1$ observation vector \mathbf{y}_t . \mathbf{w}_t and \mathbf{v}_t are the error terms with means of zero and variances constrained by diagonal matrices \mathbf{Q} and \mathbf{R} , respectively, which contain the (MVN = multivariate normal) error variances (Holmes et al. 2023).

Model – components used	Equations used	Assumptions
13.3.1 Observation error only (equivalent to multivariate linear regression).	$\mathbf{y}_t = \mathbf{Z}_t \mathbf{x}_t + \mathbf{a}_t + \mathbf{D}_t \mathbf{d}_t + \mathbf{v}_t$	Slopes of covariates estimated. No estimates of autoregressive terms because no state variables included.
13.4a State variable process-error-only model	$\mathbf{x}_t = \mathbf{B}_t \mathbf{x}_{t-1} + \mathbf{u}_t + \mathbf{C}_t \mathbf{c}_t + \mathbf{w}_t$	Diagonal of \mathbf{Q} fixed. Includes autoregressive terms
13.4b State variable process-only model – a mean-reverting model	$\mathbf{x}_t = \mathbf{B}_t \mathbf{x}_{t-1} + \mathbf{u}_t + \mathbf{C}_t \mathbf{c}_t + \mathbf{w}_t$	Diagonal of \mathbf{Q} unequal. Includes autoregressive terms
13.4c State variable process-only model – a mean-reverting model with initial values of \mathbf{x} at time 0 determined by the data matrix.	$\mathbf{x}_t = \mathbf{B}_t \mathbf{x}_{t-1} + \mathbf{u}_t + \mathbf{C}_t \mathbf{c}_t + \mathbf{w}_t$	Diagonal of \mathbf{Q} unequal. Includes autoregressive terms. \mathbf{x} at time zero estimated from observed snail counts.
13.5a Both process- and observation model – covariates only affect the state variables	$\mathbf{x}_t = \mathbf{B}_t \mathbf{x}_{t-1} + \mathbf{u}_t + \mathbf{C}_t \mathbf{c}_t + \mathbf{w}_t$ $\mathbf{y}_t = \mathbf{Z}_t \mathbf{x}_t + \mathbf{a}_t + \mathbf{v}_t$	Covariates do not affect observation terms
13.5b Both process- and observation model – the covariates only affect the observation variables:	$\mathbf{x}_t = \mathbf{B}_t \mathbf{x}_{t-1} + \mathbf{u}_t + \mathbf{w}_t$ $\mathbf{y}_t = \mathbf{Z}_t \mathbf{x}_t + \mathbf{a}_t + \mathbf{D}_t \mathbf{d}_t + \mathbf{v}_t$	Covariates do not affect state variable terms

*The covariate coefficient (‘slope’ estimates from models in table rows above 13.3.1 and 13.4c are those presented in Tables 1 and 2 in the main article, respectively. Note that t represents the year, **bold font** denotes matrices or vectors and it is assumed that the error variances have a MVN (multivariate normal distribution).

Table S4. Descriptive statistics and abbreviations ^a of raw oceanographic and environmental variables compiled using custom R scripts to compute monthly mean values for 1994 and 2021, unless otherwise specified ^{b-f}.

Variable	Minimum	Maximum	Mean	SE	SD	Months
Mean airT Tofino ^b °C	3.15	16.98	10.193	0.2186	3.837	336
Extr Min airT Tofino ^b °C	-10	10.2	1.8139	0.25432	4.463	336
Extr Max airT Tofino ^b °C	9.1	31.2	18.4133	0.3281	5.758	336
Mean SST LP Buoy ^c °C	6.0	18.2	11.17	0.02283	2.2546	336
Min SST LP Buoy ^c °C	5.4	17.9	10.76	0.0215	2.1229	336
Max SST LP Buoy ^c °C	6.0	19.9	11.71	0.02554	2.5215	336
VCMX_wave LPBuoy ^c m	0	22.6	3.73	2.07	0.0044	336
WindSPD LP Buoy ^c m.s ⁻¹	0	22.7	5.63	3.62	0.0078	336
Rain daily CB ^d (mm)	0	191.6	7.603	0.14099	13.669	336
Min_airT CB ^d °C	-7.5	17.5	7.225	0.0388	3.7608	336
Max_airT CB ^d °C	-1.0	30.0	12.486	0.0402	3.9021	336
January surface current direction degrees from North (0° or 360°) ^e	3.69 N	353.99 N	299.51 WNW	33.80	106.9	20
July surface current direction degrees from North (180°) ^e	165.96 SSE	225.91 WSW	188.6 S	5.945	18.80	20
January surface current speed ^e cm.s ⁻¹	16	38	29.6	2.437	7.706	20
July surface current speed ^e cm.s ⁻¹	8	45	24.7	3.138	9.922	20
Folger Pinnacle °C 25 m ^f	6.73	15.4	9.77	0.1359	1.238	83
Folger Deep °C 96 m ^f	7.22	12.8	8.76	0.0795	0.9269	136

^a CB = Cape Beale Lighthouse, Extr = extreme, LP = La Perouse Buoy, SPD = speed, SST = sea surface temperature, STP = sea surface temperature from LP buoy, T = temperature, Tofino = Tofino airport weather station, tot = total, VCMX = maximum wave height at LP buoy, WindSPD = windspeed from LP buoy.

^b Environment Canada Tofino Airport summarised monthly from hourly data (Fig. 1 in the main article, Table S2).

^c From Buoy C46206 - La Perouse Bank summarised monthly from hourly data (Fig. 1 in the main article, Table S2).

^d Canadian Coast Guard Cape Beale Light Station summarised monthly from daily data (Fig. 1 in the main article, Table S2).

^e Real-Time Surface Currents produced by the HF-Radar Network Stations averaged for January and for July from 2012 to 2021 (N = 20, Table S2).

^f Ocean Networks Canada's underwater cable observatory platform at Folger Passage Pinnacle 25 m: 2013–2021 and Folger Passage Deep 100 m: 2009–2021 (Table S2, Fig. 1 in the main article, S2).

Table S5. Pearson correlations between the yearly anomalies in Hadley Sea Surface Temperature (SST)^a and the yearly anomalies in environmental^b or oceanographic^{a,c,d} variables illustrate the collinearity problem of environmental temperature covariates. All abbreviations^c

Hadley SST ^a correlation with:	r	N	P uncorrected
Reynolds SST ^a	0.919	31	<0.00001
NASA-satellite chlorophyll ^a	0.378	21	0.091
Hadley_EN4 Salinity 5 m ^a	-0.200	30	0.289
ICOADS scaler windspeed ^a	-0.857	31	<0.00001
Mean air temp Tofino ^b	0.919	26	<0.00001
Extr min air temp Tofino ^b	0.499	26	0.009
Extr max air temp Tofino ^b	0.656	26	0.000274
Mean SST LaPerouse Buoy ^c	0.838	31	<0.00001
Min SST LaPerouse Buoy ^c	0.869	31	<0.00001
Max SST LaPerouse Buoy ^c	0.540	31	0.002
Mean WSPD LaPerouse Buoy ^c	-0.388	31	0.031
Min WSPD LaPerouse Buoy ^c	-0.239	30	0.203
Max WSPD LaPerouse Buoy ^c	-0.318	31	0.082
Mean VCMX LaPerouse Buoy ^c	0.412	31	0.021
Min VCMX LaPerouse Buoy ^c	0.009	31	0.963
Max VCMX LaPerouse Buoy ^c	0.148	31	0.427
Rainfall mean daily Cape Beale ^d	0.346	26	0.083
Rainfall Emax daily Cape Beale ^d	0.303	26	0.132
Mean daily min air temp Cape Beale ^d	0.636	26	0.000479
Mean daily max air temp Cape Beale ^d	0.912	26	<0.00001

^a Satellite databases and products compiled by NOAA’s NAUPLIUS Spatiotemporal Data Toolkit using the 1992–2021 baseline to calculate mean climatology except for chlorophyll, which used 1998–2021 (Fig. 1 in the main article, Table S2).

^b Environment Canada Tofino airport weather station (Fig. 1 in the main article, Table S2).

^c Canadian Coast Guard Buoy C46206 - La Perouse Bank, Barkley Sound (Fig. 1 in the main article, Table S2).

^d Canadian Coast Guard Cape Beale Light Station (Fig. 1 in the main article, Table S2).

^e Abbreviations: CB = Cape Beale Lighthouse, Extr = extreme, LP = La Perouse Buoy, SPD = speed, SST = sea surface temperature, STP = sea surface temperature from LP buoy, T = temperature, Tofino = Tofino airport weather station, VCMX = maximum wave height in metres at LP buoy.

Table S6. Subsets of covariates tried for small (<3.5 mm shell length) *Littorina scutulata sensu lato* (smsc) with the best-fitting MARSS *state variables only* model (Table S3, model 13.4c) with log10 snail count anomalies from both sites: PP and NP fit simultaneously but those for each season fit separately. All abbreviations ^a

Species	Season	Covariates	Rank	AICc (July)	ΔAICc (82.4)
smsc (Table 1, S9)	July	SST_Feb, SST_Aug, PACHY_Jul	1	82.4	0.0
smsc	July	SST_Feb, SST_Aug, CB meanmax air Jul, PACHY Jul	2	82.9	0.5
smsc	July	SST_Feb, SST_Aug, CB_meanmax_air_Jul, PACHY_Jul, WDSP_Jul_ICODS	3	83.6	+1.2
smsc	July	SST_Feb, SST_Aug	4	85.3	+2.9
smsc	July	SST_Feb, PACHY_Jul	5	87.4	+5.0
smsc	July	SST_Feb, SST_Aug, CB meanmin air Jul	6	88.9	+6.5
smsc	July	SST_Feb, SST_Aug, CB meanmin air Jul, Windspeed_Jul_ICODS	7	89.0	+6.6
smsc	July	SST_Feb, Salinity_Jul	8	91.1	+8.7
smsc	July	SST_Feb, VCARbuoy_Jul, WSPDbuoy_Jul, PACHY_Jul	9	91.9	+9.5
smsc	July	SSTbuoy_Feb, PACHY_Jul	10	97.5	+15.1
smsc	July	SSTbuoy_Feb, Salinity_Jul	11	98.2	+15.8
smsc	July	SSTbuoy_Feb, PP_smsub_JL, NP_smsub_JL	12	98.8	+16.4
smsc	July	SST_Feb, SST_Jul, Salinity_Jul, CB_daily_rain_Jul, PACHY_Jul	13	99.5	+17.1
smsc	July	SSTbuoy_Feb, Salinity_Jul, CB meanmax air Jul	14	102.7	+20.3
smsc	July	SST_Feb, VCARbuoy_Jul, WSPDbuoy_Jul, PACHY_Jul, PPlgsubJL, NPPlgsubJL	15	103.7	+21.3

Species	Season	Covariates	Rank	AICc (December)	ΔAICc (110.8)
smsc (Table 1, S9)	December	SST_Feb, SST_Aug	1	110.8	0.0
smsc	December	SST_Feb, SST_Aug, PACHY_Jul	2	111.5	+0.7
smsc	December	SST_Feb, SST_Aug, SST_Dec	3	113.0	+2.2
smsc	December	SST_Feb, SST_Aug, CB_daily_rain_Jul, PACHY_Jul	4	115.4	+4.6
smsc	December	SST_Feb, PACHY_Jul	5	115.6	+4.8
smsc	December	SST_Feb, SST_Aug, CB_meanmax_air_Jul, PACHY_Jul	6	116.7	+5.9
smsc	December	SST_Feb, Salinity_Jul	7	118.6	+7.8
smsc	December	SST_Feb, VCARbuoy_Jul	8	119.2	+8.4
smsc	December	SSTbuoy_Feb, PACHY_Jul	9	122.6	+11.8
		SST_Feb, SST_Aug, CB_meanmax_air_Jul, PACHY_Jul, WDSP_Jul_ICODS	10	123.5	+12.7
smsc	December	SSTbuoy_Feb, Salinity_Jul	11	125.5	+14.7

smsc	December	SSTbuoy_Feb, PP_smsub_Dec, NP_smsub_Dec	12	128.2	+17.4
smsc	December	SSTbuoy_Feb, Salinity_Jul, CB_meanmax_air_Jul	13	129.7	+18.9

^a AICc Akaike’s Information Criterion corrected for small sample size, Aug = August, CB = Cape Beale Lighthouse, CL = Confidence limits, DD = direct developing from egg mass, Dec = December, Feb = February, ICODS = International Comprehensive Ocean-Atmosphere Data Set, Jul = July, LP = La Perouse Buoy, MARSS = multivariate autoregressive state space model, max = maximum, min = minimum, N/A = not applicable to this group because season does not match, NP = Nudibranch Point study site, PACHY = counts of counts of the lined shore crab (*Pachygrapsus crassipes*), PD = planktonic developing from floating egg capsule, PP = Prasiola Point study site, sm = small size class of snails with shell length between 1.5 and 3.4 mm, snails = *Littorina* spp., SPD = speed, SST = sea surface temperature, SSTbuoy = sea surface temperature from La Perouse moored buoy, sub = *L. subrotundata*, sc = *L. scutulata sensu lato*, which represents *L. scutulata sensu stricto* and *L. plena* combined counts, T = temperature, WSPD = scalar windspeed from ICODS, ?? = wild card for snail species abbreviation with different life history type as covariate.

Table S7. Subsets of covariates tried for small (<3.5 mm shell length) *Littorina subrotundata* (smsub) with chosen MARSS *state variables only* model (Table S3, model 13.4c) with log10 snail count anomalies from both sites: PP and NP fit simultaneously but those for each season fit separately. All abbreviations ^a

Species	Season	Covariates	Rank	AICc (July)	ΔAICc (124.9)
smsub (Table 1, S9)	July	SSTbuoy_Feb, Salinity_Jul	1	124.9	0
smsub	July	SST_Feb, Salinity_Jul	2	125.9	+1
smsub	July	SSTbuoy_Feb, Salinity_Jul, CB_meanmax_air_Jul	3	126.2	+1.3
smsub	July	SST_Feb, CB_meanmax_air_Jul	4	128.6	+3.7
smsub	July	SSTbuoy_Feb, PACHY_Jul	5	128.7	+3.9
smsub	July	SST_Feb, PACHY_Jul	6	130.1	+5.2
smsub	July	SST_Feb, CB_meanmax_air_Jul, PACHY_Jul	7	132.2	+7.3
smsub	July	SST_Feb, SST_Aug	8	132.3	+7.4
smsub	July	SST_Feb, SST_Aug, PACHY_Jul	9	135.8	+10.9
smsub	July	SST_Feb, SST_Aug, CB_meanmax_air_Jul, PACHY_Jul	10	137.7	+12.8
smsub	July	SST_Feb, SST_Jul, Salinity_Jul, CB_daily_rain_Jul, PACHY_Jul	11	138.0	+13.1
smsub	July	SSTbuoy_Feb, PPsmcJL, NPsmcJL	12	138.6	+13.7
smsub	July	SST_Feb, SST_Aug, CB_meanmax_air_Jul, PACHY_Jul, WDSP_Jul_ICODS	13	142.5	+17.6

Species	Season	Covariates	Rank	AICc (December)	ΔAICc (140.0)
smsub (Table 1, S9)	December	SSTbuoy_Feb, Salinity_Jul, CB_meanmax_air_Jul	1	140.0	0
smsub	December	SSTbuoy_Feb, Salinity_Jul	2	140.3	+0.3
smsub	December	SSTbuoy_Feb, PACHY_Jul	3	140.8	+0.8
smsub	December	SSTbuoy_Feb, smsc_PP_Dec, smc NP_Dec	4	141.0	+1.0
smsub	December	SST_Feb, CB_meanmax_air_Jul	5	141.3	+1.3
smsub	December	SST_Feb, Salinity_Jul	6	145.2	+5.2
smsub	December	SST_Feb, SST_Aug	7	146.9	+6.9
smsub	December	SST_Feb, PACHY_Jul	8	147.4	+6.6
smsub	December	SST_Feb, SST_Aug, SST_Dec	9	151.9	+11.9
smsub	December	SST_Feb, SST_Aug, PACHY_Jul	10	152.5	+12.5
smsub	December	SST_Feb, SST_Aug, CB_meanmax_air_Jul, PACHY_Jul,	11	152.9	+12.9
smsub	December	SST_Feb, SST_Aug, CB_meanmax_air_Jul, PACHY_Jul, WDSP_Jul_ICODS	12	158.2	+18.2
smsub	December	SST_Feb, SST_Aug, CB_daily_rain_Jul, PACHY_Jul	13	158.6	+18.6

^a AICc Akaike’s Information Criterion corrected for small sample size, Aug = August, CB = Cape Beale Lighthouse, CL = Confidence limits, DD = direct developing from egg mass, Dec = December, Feb = February, ICODS = International Comprehensive Ocean-Atmosphere Data Set, Jul = July, LP = La Pouse Buoy, MARSS = multivariate autoregressive state space model, max = maximum, min = minimum, N/A = not

applicable to this group because season does not match, NP = Nudibranch Point study site, PACHY = counts of the lined shore crab (*Pachygrapsus crassipes*), PD = planktonic developing from floating egg capsule, PP = Prasiola Point study site, sm = small size class of snails with shell length between 1.5 and 3.4 mm, snails = *Littorina* spp., SPD = speed, SST = sea surface temperature, SSTbuoy = sea surface temperature from La Perouse moored buoy, sub = *L. subrotundata*, sc = *L. scutulata sensu lato* which represents *L. scutulata sensu stricto* and *L. plena* combined counts, T = temperature, WSPD = scalar windspeed from ICODS, ?? = wild card for snail species abbreviation with different life history type as covariate.

Table S8. Subsets of covariates tried for the chosen MARSS *state variables only* model (Table S3, model 13.4c) with log10 snail count anomalies when both sites: PP and NP and both species: smsc and smsub were fit simultaneously as dependent variables. All abbreviations ^a

Species	Season	Covariates	Model (MARSS)	AICc (July)	ΔAICc (82.9, 124.9)
both	July	SST_Feb, SST_Jul, Salinity_Jul, CB_daily_rain_Jul, PACHY_Jul	2 (=13.4c)	244.3	+119.4 +161.4
both	July	SST_Feb, SST_Jul, Salinity_Jul, CB_daily_rain_Jul, CB_meanmax_air_Jul, PACHY_Jul	2 (=13.4c)	254.5	+124.6, +171.6
				AICc (December)	ΔAICc (110.8, 140.8)
both	December	SST_Feb, SST_Aug, CB_daily_rain_Aug, PACHY_Jul	2 (=13.4c)	275.9	+135.1 +165.1
both	December	SST_Feb, SST_Dec, CB_meanmax_air_Aug, CB_daily_rain_Aug, PACHY_Jul	2 (=13.4c)	278.3	+137.5 +167.5
both	December	SST_Feb, SST_Aug, SST_Dec, CB_daily_rain_Aug, PACHY_Jul	2 (=13.4c)	288.3	+163.4 +205.4

^a AICc Akaike’s Information Criterion corrected for small sample size, Aug = August, CB = Cape Beale Lighthouse, CL = Confidence limits, DD= direct developing from egg mass, Dec = December, Feb = February, ICODS = International Comprehensive Ocean-Atmosphere Data Set, Jul = July, LP = La Perouse Buoy, MARSS = multivariate autoregressive state space model, max = maximum, min = minimum, N/A = not applicable to this group because season does not match, NP = Nudibranch Point study site, PACHY = counts of counts of the lined shore crab (*Pachygrapsus crassipes*), PD = planktonic developing from floating egg capsule, PP = Prasiola Point study site, sm = small size class of snails with shell length between 1.5 and 3.4 mm, snails = *Littorina* spp., SPD = speed, SST = sea surface temperature, SSTbuoy = sea surface temperature from La Perouse moored buoy, sub = *L. subrotundata*, sc = *L. scutulata sensu lato* which represents *L. scutulata sensu stricto* and *L. plena* combined counts, T = temperature, WSPD = scalar windspeed from ICODS, ?? = wild card for snail species abbreviation with different life history type as covariate.

Table S9. Comparative rank and AICc values for different subsets of covariates based on the fit of the log10 count anomalies of small snails to the best MARSS *state–variable* model (Table S3, model 13.4c) with both study sites (PP and NP) being fit simultaneously. Four life history types: (PD or DD) by season (July or December) groupings of small snails were compared. Only subsets of covariates with a Δ AICc value of <5.0 for at least one life history by season grouping model run are shown here. See Tables S6–S8 for rank and Δ AICc values of all subsets of covariates tried for this model. All abbreviations ^a

Covariates	PD-July	DD-July	PD-December	DD-December
SST_Feb, SST_Aug, PACHY_Jul	#1 (82.4)	#9 (135.8)	#2 (111.5)	#10 (152.5)
SSTbuoy_Feb, Salinity_Jul	#11 (98.2)	#1 (124.9)	#11 (125.5)	#2 (140.3)
SST_Feb, SST_Aug	#4 (85.3)	#8 (132.3)	#1 (110.8)	#7 (146.9)
SSTbuoy_Feb, Salinity_Jul, CB_meanmax_air_Jul	#14(102.7)	#3 (126.2)	#13 (129.7)	#1 (140.0)
SSTbuoy_Feb, PACHY_Jul	#10 (97.5)	#5 (128.7)	#9 (122.6)	#3 (140.8)
SST_Feb, SST_Aug, CB_meanmax_air_Jul, PACHY_Jul	#2 (82.9)	#10 (137.7)	#6 (116.7)	#11 (152.9)
SST_Feb, SST_Aug, CB_meanmax_air_Jul, PACHY_Jul, WDSP_Jul_ICODS	#3 (83.6)	#13 (142.5)	#10 (123.5)	#12 (158.2)
SST_Feb, Salinity_Jul	#8 (91.1)	#2 (125.9)	#7 (118.6)	#6 (145.2)
SST_Feb, SST_Aug, SST_Dec	N/A	N/A	#3 (113.0)	#9 (151.9)
SST_Feb, SST_Aug, CB_daily_rain_Jul, PACHY_Jul	N/A	N/A	#4 (115.4)	#13 (158.6)
SST_Feb, PACHY_Jul	#5 (87.4)	#6 (130.1)	#5 (115.6)	#8 (147.4)
SSTbuoy_Feb, PP_sm??_Jul, NP_sm??_Jul	#9 (98.8)	#12 (138.6)	N/A	N/A
SSTbuoy_Feb, PP_sm??_Dec, NP_sm??_Dec	N/A	N/A	#12 (128.2)	#4 (141.0) ^b

^a AICc Akaike’s Information Criterion corrected for small sample size, Aug = August, CB = Cape Beale Lighthouse, CL = Confidence limits, DD= direct developing from egg mass, Dec = December, Feb = February, ICODS = International Comprehensive Ocean-Atmosphere Data Set, Jul = July, LP = La Perouse Buoy, MARSS = multivariate autoregressive state space model, max = maximum, min = minimum, N/A = not applicable to this group because season does not match, NP = Nudibranch Point study site, PACHY = counts of counts of the lined shore crab (*Pachygrapsus crassipes*), PD = planktonic developing from floating egg capsule, PP = Prasiola Point study site, sm = small size class of snails with shell length between 1.5 and 3.4 mm, snails = *Littorina* spp., SPD = speed, SST = sea surface temperature, SSTbuoy = sea surface temperature from La Perouse moored buoy, sub = *L. subrotundata*, sc = *L. scutulata sensu lato*, which represents *L. scutulata sensu stricto* and *L. plena* combined counts, T = temperature, WSPD = scalar windspeed from ICODS, ?? = wild card for snail species abbreviation with different life history type as covariate.

^b Slopes for PD small snail covariates were significantly positive for PP: X.smsub_PP_Dec, smsc_PP_Dec: 0.560 (0.01939, 1.10) but were not significant for NP for X.smsub_NP_Dec, smsc_NP_Dec: 0.224 (–0.339, 0.787) because the 95% CL overlapped zero.